

# Simulation of CVD Process in a Reactor

A. Kulkarni, V. Frettlöh

Gemeinnützige KIMW Forschungs-GmbH, Lüdenscheid, NRW, Germany

## Introduction

Steel tools, which are used in industrial high-throughput processes like injection molding, are susceptible for wear and corrosion due to rapid cyclic temperature and pressure fluctuation as well as the use of abrasive polymers. For the protection of tool surfaces high quality ceramic thin films can be applied by metal-organic chemical vapor deposition (MOCVD) [1]. In addition to protective properties ceramic materials like yttria-stabilized zirconia (YSZ) are able to thermally insulate tool surfaces providing a more precise temperature regulation with intent to avoid the formation of surface flaws, e.g. weld lines, in the fabricated plastic parts. At the same time it enables the shortening of cycle times as well as the decrease of energy demands during the molding process [2]. In our work we demonstrate the fabrication of zirconia based thin films on steel tools with complex 3D surfaces via MOCVD using zirconium acetylacetonate as precursor material. Compared with other coating techniques CVD enables a homogeneous layer thickness distribution even on highly complex surface geometries [3]. The main aim of this work is to find out the optimum position for the test specimens in the reactor so that the coating on the specimen is homogeneous. The influence of gas flow, temperature, and pressure on the flow behavior within the reactor and around and through a demonstrator tool can be simulated with Comsol Multiphysics.

## Theory / Experimental Set-up

For the coating of the specimen as well as the tool inserts for injection molding tools a hot wall CVD reactor is used. In order to coat common steels without losing their mechanical strength the coating process takes place at temperatures below 500°C.

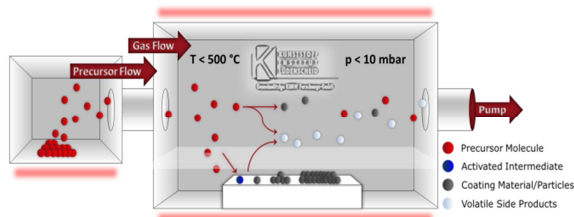


**Figure 1:** Schematic representation of the CVD reactor and process (gemeinnuetzige KIMW Forschungs-GmbH)

We use metal-organic precursors decomposing in-situ under higher temperatures to be able to achieve the, compared to the traditional CVD, relatively low coating temperatures. The precursor, a volatile molecular compound, is evaporated and led into the reaction chamber, which is at small vacuum. In there, a thermal induced decomposition reaction takes place during which the precursor is first adsorbed on the surface where it reacts to the desired material and thus completes the deposition process.

The coating material itself is generated by specific chemical reactions, so understanding of physical and chemical mechanisms inside the chamber is necessary to develop a process. Properties of the chosen material depend, beside the material itself, mainly upon the process parameters temperature, pressure, gas flow and precursor flow, which can be varied. The precursor material is evaporated in an evaporator and transferred through the main nozzle into the reactor volume by a carrier gas. To homogenize the gas flow, the same amount of gas is additionally transferred into the reactor through several smaller nozzles arranged circular around the main nozzle (ring nozzles).

To analyze the 3D conformity and the groove penetration properties of the coating, different kinds of demonstrator tools can be used. For this work we used a rectangular tool with a cylindrical hole and four breakthroughs on the upper side, in which small metal round blanks can be placed. With this demonstrator the coating thickness within the demonstrator can be measured by measuring the coating thickness on the metal round blanks. The demonstrator can be surrounded by metal plates to force nearly the whole gas to stream through the demonstrator and no longer also around it.



**Figure 2:** Demonstrator tool without (left) and with (right) metal plates

The coating should be homogenous along the whole inner surface of the demonstrator to achieve an

optimal functionalized tool surface with the same properties independent of the position on the tool.

The coating thickness on the metal round blanks was analyzed by calotte grinding and measuring the calotte radius with help of a microscope.

The coating processes presented in this paper were realized at 385 °C and a pressure of 5 mbar (500 Pa). The tool geometry (with and without plates around the demonstrator tool) as well as the amount of gas flow were varied during the session of processes.

The CVD reactor itself is made of ceramic and heated by an external oven. The actual coating takes place within a tube made of steel. The oven is isolated from the outer surface, so that the ceramic tube outside the oven becomes also hot but is simultaneously cooled by the surrounding air so that it does not show such high temperatures. In order to realize a proper coating the oven is heated with a certain temperature gradient.



**Figure 3:** CVD reactor at the gemeinnuetzige KIMW Forschungs-GmbH

### Governing Equations

With the help of COMSOL Multiphysics it was relatively straightforward to imply the gas flow simulation within the reactor present at

gemeinnuetzige KIMW Forschungs-GmbH. The CFD module was used to carry out all the simulations. The type of flow considered for simulations is based on the Reynolds number which gives us an idea if the flow is laminar or turbulent. From the experimental data of pressure and gas flow rate it was clear that for this problem laminar flow should be taken into consideration. Laminar flow is based on the Navier-Stokes equation:

$$\rho \left( \frac{\partial \mathbf{u}}{\partial t} + (\mathbf{u} \cdot \nabla) \mathbf{u} \right) = -\nabla p + \nabla \cdot \left[ \mu \left( \nabla \mathbf{u} + (\nabla \mathbf{u})^T - \frac{2}{3} (\nabla \cdot \mathbf{u}) \mathbf{I} \right) \right] + \mathbf{F}$$

$$\frac{\partial p}{\partial t} + \nabla \cdot (\rho \mathbf{u}) = 0$$

$$\rho = \rho(p, T)$$

Where,

- $\mathbf{u}$  = Velocity of fluid
- $\rho$  = Density of fluid
- $p$  = Pressure of fluid
- $\mu$  = Dynamic viscosity
- $T$  = Temperature of fluid
- $\mathbf{F}$  = External body forces
- $\mathbf{I}$  = Identity tensor

The equation shows that the density is dependent on the pressure and temperature of the fluid. In Comsol one can define self-required variables depending on the equations. For the processes taken into account for experiments, the pressure considered is varied from 100 to 500 Pa. So every time the pressure is varied, it becomes necessary to calculate the density. This was simplified by defining the equation for the variable 'rho' for density and then later on considered in a parametric sweep which is used to vary the pressure and temperature for this case.

**Table 1:** Overview about the layer growth rates on the specimen depending of the gas flow and the demonstrator geometry. The temperature for all coating experiments was 385 °C, the pressure within the reactor was retained at 5 mbar (500 Pa); specimen 1 is closest to the nozzle.

Process	Sample geometry	Gas flow main nozzle / ring nozzles (sccm)	Layer growth rate (µm/h) on the specimen 1-4				Average growth rate (µm/h)
1	without plates	450 / 450	0.31	0.29	0.26	0.23	0.27
2	with plates	450 / 450	0.23	0.20	0.19	0.18	0.20
3	with plates	125 / 125	0.86	0.68	0.62	0.48	0.66

**Table 2:** Overview about the simulation parameters used

Process	Sample geometry	Temperature (°C)	Pressure (Pa)	Gas flow main nozzle / ring nozzles (sccm)
1	without plates	385	500	450 / 450
2	with plates	385	500	450 / 450
3	with plates	385	500	125 / 125

## Experimental Results

Regarding the demonstrator without the plates, the gas can flow through the specimen as well as around the demonstrator. The flow pattern on the coated metal round blanks showed a real good gap penetration capability since the coating is not only visible on the part directly in contact with the inner surface of the demonstrator tool but also on the areas which are covered by the metal of the demonstrator tool holding the metal plates in position (Figure 4).



**Figure 4:** Specimen coated in the demonstrator *without plates* at 385°C, 500 Pa and with gas flows of 450 sccm (main nozzle) and 450 sccm (ring nozzles)

Concerning the case for the demonstrator tool without the plates the coating growth rate showed an average over all four specimen of 0.27  $\mu\text{m}/\text{h}$ . But the gradient from the first to the last plate within the demonstrator was 0.08  $\mu\text{m}$  (process 1, Table 1).

The metal plates coated in the demonstrator tool with plates (process 2, Table 1) showed a different flow pattern. The gap penetration capability is worse and the growth rate on the specimen is a bit lower compared to process 1. Though the layer growth gradient from the first to the last specimen is with 0.05  $\mu\text{m}$  lower as in process 1, so the coating homogeneity is higher (Figure 5).

Due to the higher gas velocity it might be that the molecules do not have enough time to react with the metal surface, so that the coating growth rate decreased.



**Figure 5:** Specimen coated in the demonstrator *with plates* at 385°C, 500 Pa and with gas flows of 450 sccm (main nozzle) and 450 sccm (ring nozzles)

As seen in the simulations, the gas velocity within the demonstrator tool is seven times higher with plates than without plates. A reduction of the gas flow might therefore lead to an even better coating growth rate. A third process was therefore realized with lower gas flow rates but under conservation of the temperature and pressure of the first two processes.

One of the coated specimens is shown in Figure 6. The higher coating thickness becomes apparent due to the significant darker coating appearance. The growth rate for this process is threefold higher than for the previous mentioned specimen (process 3, Table 1), but the gap penetration ability is worse, since the metal round blanks do not show any flow pattern on the side areas supported by the demonstrator material.



**Figure 6:** Specimen coated in the demonstrator *with plates* at 385°C, 500 Pa and with gas flows of 125 sccm (main nozzle) and 125 sccm (ring nozzles)

Also the gradient of the growth rate from the first to the last specimen is with 0.38  $\mu\text{m}$  a lot higher than in the other two processes, meaning the homogeneity of the coating within the demonstrator tool is worse. It might be the case that the main part of the precursor works of already in the first part of the reactor since the gas flow is low.

## Simulation Results

The simulation results show the flow path of gas in the reactor. One can observe the velocity distribution in the reactor from the velocity cut sections. In the inlet sections of the reactor swirls are developed due to which the velocity in the front section of the reactor is higher and as the gas passes along in the reactor it becomes laminar. Previously the experiments showed that the specimens placed in the front of the reactor showed very less coating.

This was later verified by the simulation results because the gas flow is so rapid, gas and precursor molecules have less time to react with the specimens so they do not show a homogenous coating.

Two cases are presented in this work, first demonstrator without the plates and second with the plates. The difference in the velocity streamlines can be clearly seen in Figure 7 and Figure 9, and also the velocity differences due to the volume reduction of the demonstrator with plates become obvious. Velocities obtained in the first case without plates are lower, as a result the gas and precursor molecules flow slowly through the reactor and hence we observe 3D capability and enormous groove penetration of the coating inside the demonstrator (Figure 8, Figure 10).

In the second case with plates, as the gas and precursor molecules flow through a reduced channel higher velocities are observed and hence the coating on the specimens is lower (Figure 9, Figure 10). By reducing the amount of gas, the velocity within the demonstrator can be reduced, possibly resulting in a more consistent coating with higher 3D capability while preserving resources. Hence the velocities obtained would be much lower providing enough time for the gas and precursor molecules to react with the specimens. Because of the reduced volume a higher amount of gas could be concentrated through the demonstrator thus achieving a more homogenous coating on the specimens.

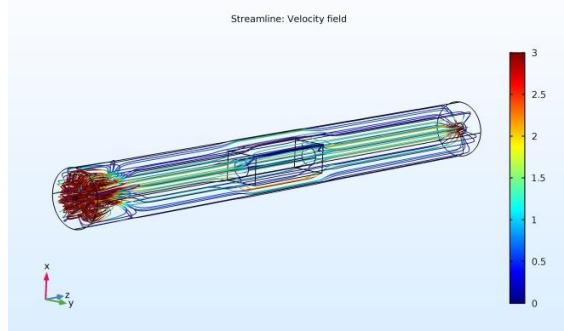


**Figure 7:** Velocity streamlines within the reactor volume with the demonstrator tool *without* plates.

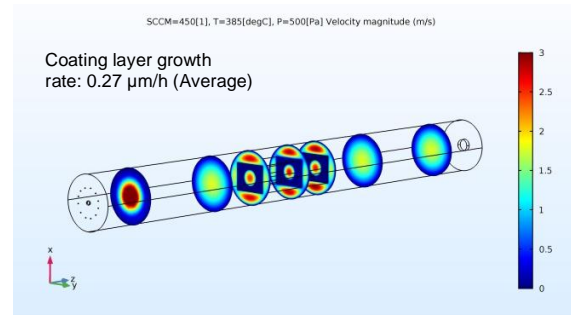


**Figure 8:** Velocity cross sections in the reactor volume with the demonstrator tool *without* plates

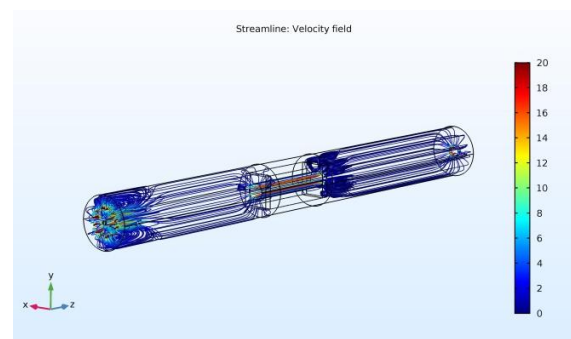


**Figure 9:** Velocity streamlines within the reactor volume with the demonstrator tool *with* plates.

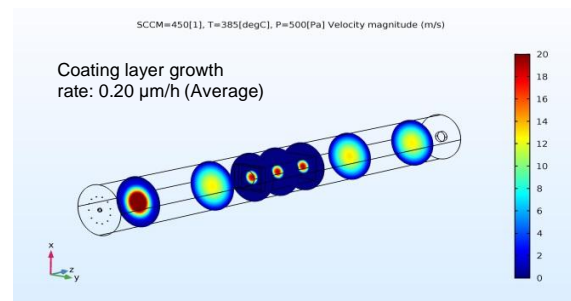


**Figure 10:** Velocity cross sections in the reactor volume with the demonstrator tool *with* plates

In order to reduce the gas velocity within the demonstrator tool, the amount of gas was reduced whereas the temperature and pressure were kept constant. The experiment was realized at the real CVD reactor (as shown above) with 125 sccm gas injected through the ring nozzles as well as through the main nozzle.

The reduced gas velocities lead (Figure 11, Figure 12) to higher coating growth rates. Since the precursor molecules have more time to react with the inner surface of the demonstrator, the coating growth rate is increased.

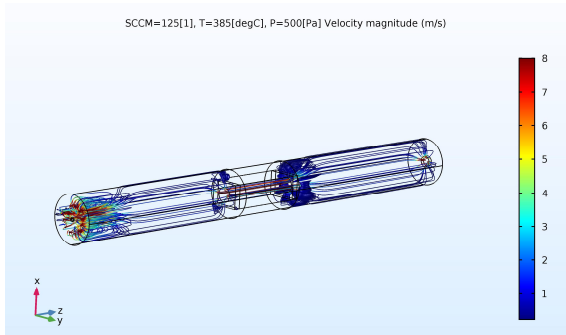


**Figure 11:** Velocity streamlines within the reactor volume with the demonstrator tool *with* plates (reduced gas flow)

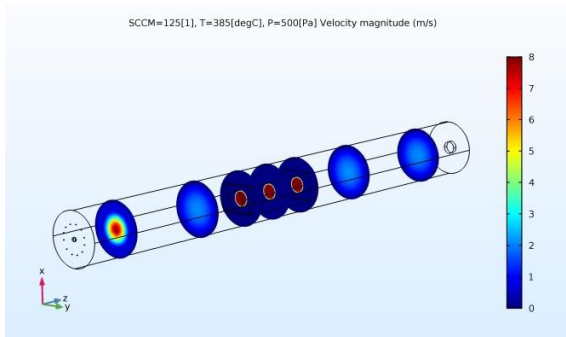


**Figure 12:** Velocity cross sections in the reactor volume with the demonstrator tool *with* plates (reduced gas flow)

For studying the temperature distributions in the CVD reactor, a heat transfer analysis was also conducted. Here we discuss the 3D model of the reactor as shown in Figure 13. The simulations show how the heat is transferred from the copper (heating elements) to the ceramic and steel cylinders. The experiments showed a better coating rate on the specimens when a temperature gradient was considered in the CVD reactor. Also at the outlet section a high temperature element was considered as it helped to decompose the precursor in a proper way. The simulation model was also build considering a temperature gradient.

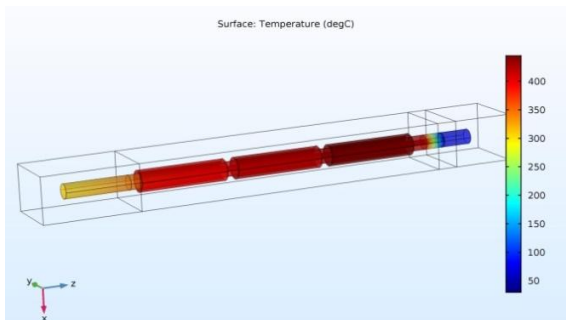


**Figure 13:** Temperatures at different sections of the reactor

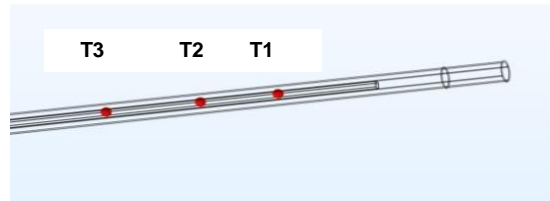


**Figure 14:** Positions of the cut points within the reactor steel tube at which the resulting temperature was considered

The temperatures were measured on the steel cylinder during the experiments at different sections on the CVD reactor and were also verified in the simulations. By optimizing the simulation model, e. g. defining a thin layer for realizing a better insulation as in the real reactor, the temperatures at three sections showed optimum values (Table 3, Figure 13).

**Table 3:** Comparison of Temperature values measured at the real CVD reactor and taken from the simulation at cut points corresponding to the position of the thermocouples in the CVD reactor

Version	T1 (°C)	T2 (°C)	T3 (°C)
Experiments	394	406	412
Simulations	392	408	421

## Conclusions

We were able to relate the simulation results with the experimental results of the CVD coating experiments. With the help of the simulations we were able to tell, which effect the reduced gas flow during the coating time might have. In order to be able to predict the coating thickness, more background information about the reactions processes during the coating process are necessary. Moreover, a rate for the deposition of the coating material on the surface has to be defined to be able to take also the chemical reactions into account. Of course the chemical reaction module might also be helpful for solving these scientific problems.

For future simulations, which mirror to a greater extent the real coating processes in the reactor, also a multiphysics simulation should be developed, in which the temperature gradient present in the CVD reactor is used and influences the gas flow through the reactor.

## References

- [1] S. Heiroth, R. Ghisleni, T. Lippert, J. Michler, A. Wokaun; Optical and mechanical properties of amorphous and crystalline yttria-stabilized zirconia thin films prepared by pulsed laser deposition; *Acta Materialia* **59**, 2330-2340 (2011).
- [2] B. Atakan, V. Khlopyanova, S. Mausberg, F. Mumme, A. Kandzia, C. Pflitsch; CVD and Analysis of thermally insulating ZrO<sub>2</sub> layers on injection molds, *Physica Status Solidi C* **12**, 878-885 (2015).
- [3] G. Fornalczyk et. al.: Yttria-Stabilized Zirconia Thin Films via MOCVD for Thermal Barrier and Protective Applications in Injection Molding, *Key Engineering Materials* **742**, 427-433, (2017).